

Electronic Supplementary Material

Monitoring nucleic acid amplification process by UiO-66-NH₂-based fluorescence sensor

Changjia Hu^{a,b}, Junbo Chen^b, Peng Yang^b, Lijie Du^b, Lingying Xia^{a,b}, Juan He^{*b}, Xiandeng Hou^{*b,c}

^aBiliary Surgical Department West China Hospital, Sichuan University Chengdu, Sichuan 610225 (China)

^bAnalytical & Testing Centre, Sichuan University, Chengdu, Sichuan 610041 (P.R. China)

^cKey Laboratory of Green Chemistry & Technology of Ministry of Education, Sichuan University, Chengdu, Sichuan 610064 (China)

E-mails: houxd@scu.edu.cn, hujuan1117@scu.edu.cn

1. Reagents and Materials

Acetic acid (HAc), potassium chloride (KCl), magnesium chloride (MgCl_2), hydrochloric acid (HCl), sodium hydroxide (NaOH), benzoic acid, anhydrous ethanol ($\text{C}_2\text{H}_5\text{OH}$) and N, N-dimethylformamide (DMF) were from Chron Chemicals Co., Ltd (Chengdu, China). Zirconium chloride (ZrCl_4), sodium hexametaphosphate ($(\text{NaPO}_3)_6$), sodium phosphite dibasic pentahydrate ($\text{Na}_2\text{HPO}_3 \cdot 5\text{H}_2\text{O}$), sodium hypophosphite monohydrate ($\text{NaH}_2\text{PO}_2 \cdot \text{H}_2\text{O}$), sodium pyrophosphate ($\text{Na}_4\text{P}_2\text{O}_7$), tri-sodium phosphate dodecahydrate ($\text{Na}_3\text{PO}_4 \cdot 12\text{H}_2\text{O}$), sodium phosphate dibasic dodecahydrate ($\text{Na}_2\text{HPO}_4 \cdot 12\text{H}_2\text{O}$), sodium phosphate monobasic dihydrate ($\text{NaH}_2\text{PO}_4 \cdot 2\text{H}_2\text{O}$) and sodium tripolyphosphate were bought from Aladdin (Shanghai, China). 2-Aminoterephthalic acid (BDC-NH₂) was from Sigma-Aldrich Trading Co. Ltd. (Shanghai, China). Tris-HCl buffer, HEPES buffer and 10×PBS buffer were commercially obtained from Sangon Biotech. Co., Ltd. (Shanghai, China). Phi 29 DNA polymerase was obtained from New England Biolabs Ltd. (Beijing, China). T4 DNA ligase, dNTP, dATP, dTTP, dCTP, and dGTP were purchased from Takara Biomedical Technology Co., Ltd. (Dalian, China). All the reagents without special mention were at least of analytical grade.

2. Apparatus

All the spectral absorption and fluorescence measurements in this work were completed by BioTek Microplate Reader (H1M, USA). Ultrapure water was from a water purification system (PCWJ-10, China). The powder X-ray diffraction (PXRD) patterns were obtained with an (X'Pert Pro MPD, Netherlands) X-ray diffraction spectrometer using $\text{Cu}_{k\alpha}$ radiation. The scanning electron microscopy (SEM) images were obtained from a field emission scanning electron microscope (JEOL JSM-7500F, Japan) at 15.00 kV.

3. DBD synthesis device

The DBD reactor (Figure S1) consisted of an open concentric quartz cylinder tube and a copper wire. A tungsten rod was embedded inside the inner cylinder as the internal electrode, and the copper wire surrounding outside of the cylinder was used as the outer electrode. When the power was on, the synthesis process began.

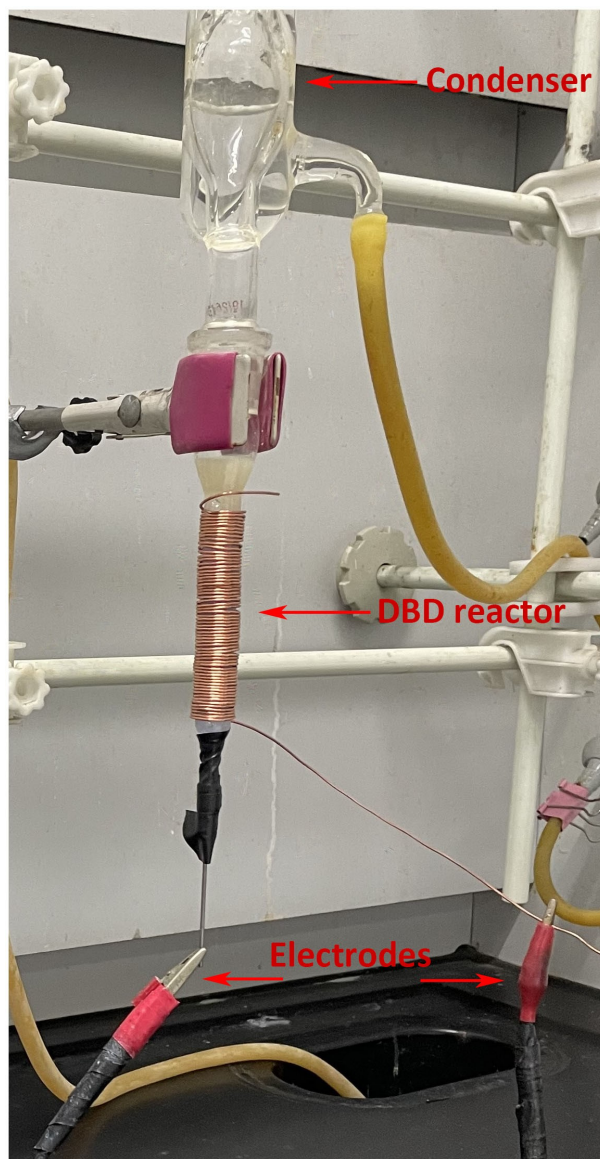


Figure S1. Photo of DBD synthesis device. Condenser, DBD reactor and electrodes are shown from top to bottom in this photo.

4. DBD plasma-induced synthesis of UiO-66-NH₂

The DBD reactor was used to synthesize UiO-66-NH₂ (Figure S2). Aliquots of 0.4 mmol of ZrCl₄, 0.4 mmol of BDC-NH₂ and 8 mmol of benzoic acid were dissolved in 6.8 mL of DMF. One drop of hydrochloric acid was added at last and mixed fully. Then, the reaction solution was transferred into the DBD reactor. After install the device required for the synthesis, turn on the power and adjust the voltage to 30 kV and current to 1.3 A to ensure the generation of the liquid-phase DBD plasma. Then, the reaction solution turned to turbid gradually, indicating the formation of the MOF product, UiO-66-NH₂. The product was removed from the DBD reactor after 30 min, centrifuged and thoroughly rinsed three times with DMF and ethanol individually. The obtained UiO-66-NH₂ was vacuum dried at 80 °C for 12 h. Finally, it was stored at room temperature and kept away from light.

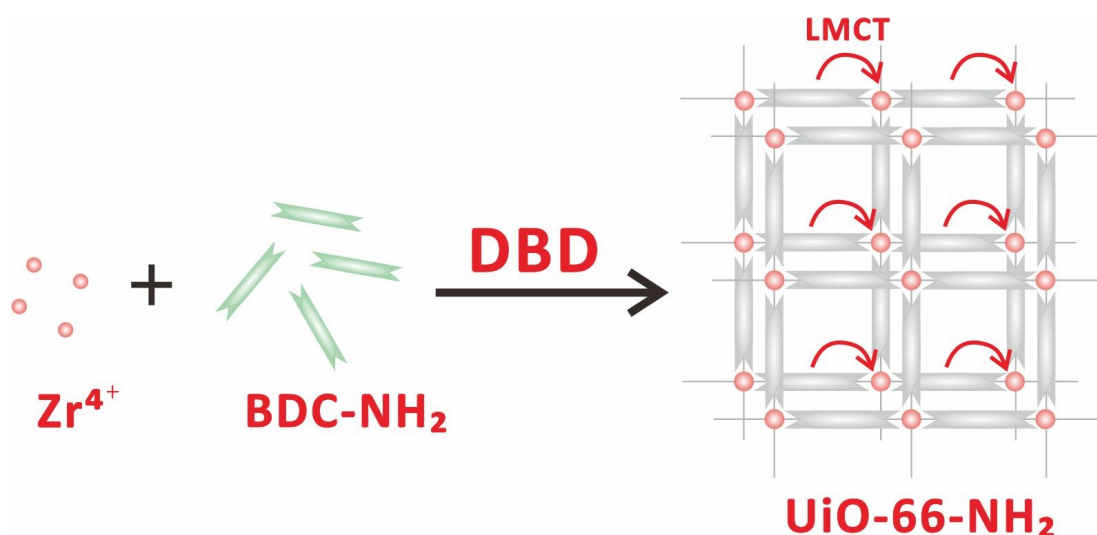


Figure S2. DBD plasma-induced synthesis of UiO-66-NH₂.

5. Comparison of PPI-responded MOFs and their synthesis

UiO-66-NH₂ was obtained by solvothermal synthesis and DBD synthesis individually. The comparison of the synthesis of UiO-66-NH₂ and other PPI-responded MOFs was listed in Table S1. It is indicated that DBD synthesis of PPI-responded UiO-66-NH₂ was much faster, easier and more convenient than others, fully showing the advantages of DBD synthesis.

Table S1. PPI-responded MOFs and their synthesis

MOFs	Methods	Dynamic range	LOD	Synthesis	Temp.	Time	Ref.
MIL-101(Cr)	Chemiluminescence	5 to 70 μ M	1.2 μ M	Reflux	>111 $^{\circ}$ C	12 h	1
Zn-TCPP(Fe)							
Co-TCPP(Fe)	Absorbance	2 to 500 μ M	-	Stirring	80 $^{\circ}$ C	24 h	2
Cu-TCPP(Fe)							
MVCM	Fluorescence	100 to 12000 μ M	55 nM	Heating	RT	>1 h	3
ZTMOF-1	Fluorescence	10 to 220 μ M	2.91 μ M	Solvothermal	115 $^{\circ}$ C	72 h	4
MOF-5-NH ₂	Fluorescence	10 to 80 μ M	0.32 μ M	Solvothermal	120 $^{\circ}$ C	21 h	5
UiO-66-N-Py	Fluorescence	1 to 1000 μ M	0.3 μ M	Solvothermal	120 $^{\circ}$ C	24 h	6
UiO-66-NH₂	Fluorescence	2 to 200 μM	0.20 μM	Solvothermal	120 $^{\circ}$C	12 h	This
UiO-66-NH₂	Fluorescence	2 to 200 μM	0.20 μM	DBD	RT	0.5 h	work

6. Solvothermal synthesis and characterization of UiO-66-NH₂

For the solvothermal synthesis of UiO-66-NH₂, aliquots of 2 mmol of ZrCl₄, 2 mmol of BDC-NH₂, 40 mmol of benzoic acid were dissolved in 34 mL of DMF. Then, mix 0.347 mL HCl with the above solution, transfer to a Teflon-lined autoclave and hold at 120 $^{\circ}$ C for 12 h. After cooling down to room temperature, the obtained product was washed and vacuum dried as in the DBD synthesis.

UiO-66-NH₂ from solvothermal synthesis was also characterized by powder X-ray

diffraction (PXRD) and scanning electron microscopy (SEM). The result of PXRD was shown as Figure 1A, and the SEM imaging indicated that the obtained products were octahedral particles with the size of about 150 nm (Figure 1B and Figure S3).

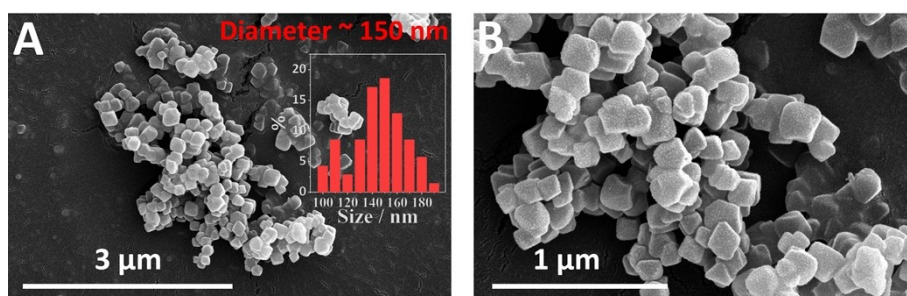


Figure S3. SEM imaging of UiO-66-NH₂ from solvothermal synthesis.

7. Dynamic light scattering (DLS) of UiO-66-NH₂

To provide a statistical analysis of UiO-66-NH₂ diameter, DLS analysis was applied and the result was shown as Figure S4. For the DBD synthesis and solvothermal synthesis of UiO-66-NH₂, DLS exhibited the main diameter of 291 nm and 254 nm, respectively. The diameter from DLS means hydrodynamic diameter, which is generally larger than particle diameter from SEM because of the presence of ligand and solvated water molecules.

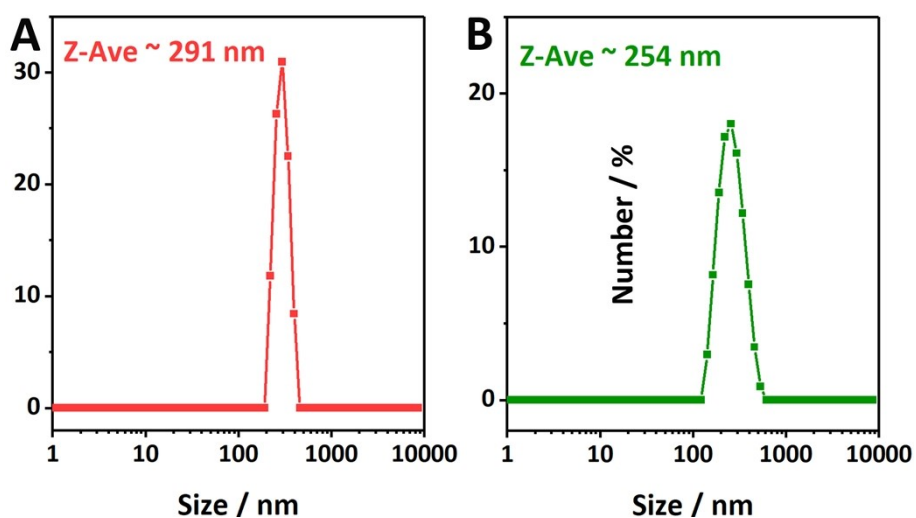


Figure S4. DLS analysis of UiO-66-NH₂ from (A) DBD synthesis and (B) solvothermal synthesis.

8. λ_{ex} and λ_{em} of UiO-66-NH₂

To test the fluorescent properties of UiO-66-NH₂, emission spectrum with excitation wavelength of 328 nm and excitation spectrum with emission wavelength of 431 nm were recorded in the range from 400 to 500 nm and 300 to 400 nm, respectively. Figure S5 exhibited that the λ_{ex} of the synthesized UiO-66-NH₂ was 330 nm and λ_{em} was 424 nm, respectively.

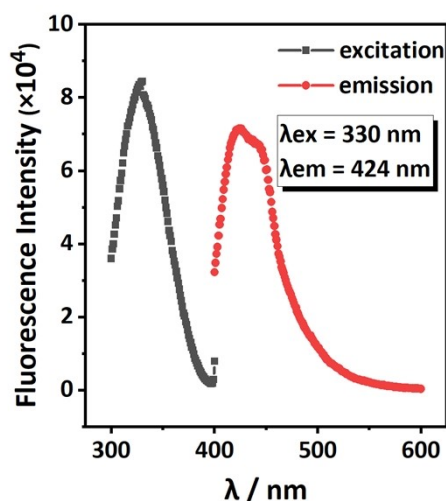


Figure S5. Excitation spectrum and emission spectrum of synthesized UiO-66-NH₂.

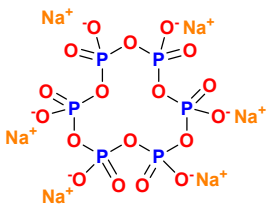


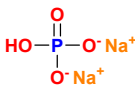
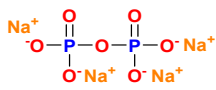
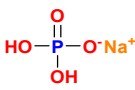
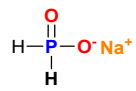
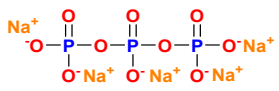
9. Sensing different phosphates by UiO-66-NH₂

For the sensing, the suspension of UiO-66-NH₂ was prepared by dispersing 1 mg of UiO-66-NH₂ in 1 mL of ultrapure water under ultrasonic conditions for 3 s. To evaluate the sensing capability of UiO-66-NH₂, different phosphates shown in Table S2, including sodium hexametaphosphate, disodium phosphite, sodium hypophosphite, sodium pyrophosphate, sodium phosphate, disodium phosphate, monosodium phosphate, sodium tripolyphosphate, dATP, dTTP, dCTP, dGTP and dNTP, were introduced to 5 μ L of UiO-66-NH₂ suspension, respectively, in which ultrapure water was also added to ensure that the total volume of the reaction was 100 μ L. Then, it was recorded their individual fluorescence intensity with the BioTek Microplate Reader.

The result in Figure S6 indicated that UiO-66-NH₂ had obvious response to these phosphates with significant fluorescence enhancement, among which sodium hypophosphite (4), dATP, dTTP, dCTP, dGTP and dNTP had much lower fluorescence intensity than other phosphates. Sodium hypophosphite (4) lacked a complete phosphate-like part, which probably attenuated the coordination with Zr cluster of

UiO-66-NH₂, causing a lower fluorescence intensity than the counterparts; and the lower fluorescence recovery of dATP, dTTP, dCTP, dGTP and dNTP might attribute to the steric effect. Moreover, phosphates mentioned above do not generally exist in the amplification system, so the interference caused by them can be ignored. For example, RCA in our work does not contain the mentioned phosphates, except PPI, so the fluorescence recovery of UiO-66-NH₂ can be an indicator of this amplification process.

Table S2. Phosphates mentioned in this work

Molecular formulas	Molecular structural formulas	Molecular formulas	Molecular structural formulas
(NaPO ₃) ₆ (1)	 <p>Sodium hexametaphosphate</p>	Na ₃ PO ₄ (5)	 <p>Sodium phosphate</p>
Na ₂ HPO ₃ (2)	 <p>Disodium phosphite</p>	Na ₂ HPO ₄ (6)	 <p>Disodium phosphate</p>
Na ₄ P ₂ O ₇ (3)	 <p>Sodium pyrophosphate</p>	NaH ₂ PO ₄ (7)	 <p>Monosodium phosphate</p>
NaH ₂ PO ₂ (4)	 <p>Sodium hypophosphite</p>	Na ₄ P ₂ O ₇ (8)	 <p>Sodium tripolyphosphate</p>

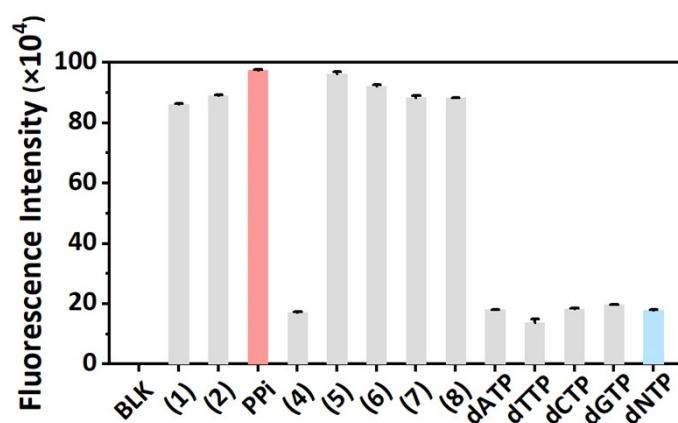
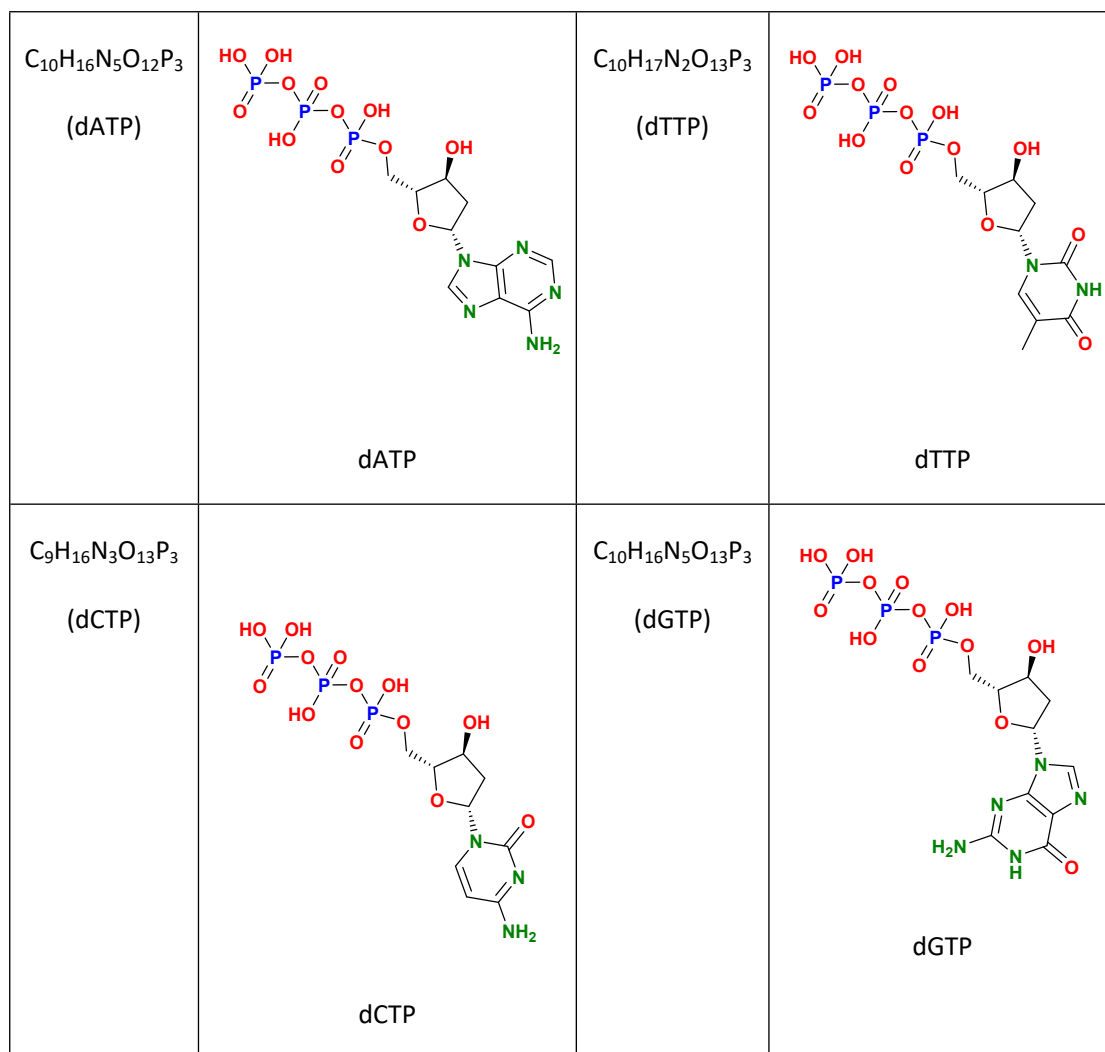


Figure S6. Fluorescence response to different phosphates of UiO-66-NH₂. The fluorescence intensity was recorded at λ_{em} (424 nm), which was excited by λ_{ex} (330 nm). The measurements were taken at 90 min and the error bar represented one standard deviation from triplicate measurements.

10. Reaction between PPI/dNTP and UiO-66-NH₂

For the detection of PPI/dNTP by UiO-66-NH₂, the PPI/dNTP solutions with different concentration (1 nM, 2 nM, 5 nM, 10 nM, 20 nM, 50 nM, 100 nM, 200 nM, 500 nM, 1 μM, 2 μM, 5 μM, 10 μM, 20 μM, 50 μM, 100 μM, 200 μM, 500 μM, 1 mM, 2 mM, 5 mM, and 10 mM) were mixed to 5 μL of the above UiO-66-NH₂ suspension and appropriate ultrapure water to make the total volume of solution 100 μL, respectively, and the fluorescence intensity was recorded with the BioTek Microplate Reader with λ_{ex} and λ_{em} at 330 nm and 424 nm, respectively.

11. Monitoring of RCA process by UiO-66-NH₂

For RCA process, the circular template (CT) was prepared first. Briefly, 2 μL of 100 μM Template (200 pmol) was mixed with varied moles of HCV (0 pmol, 2 pmol, 10 pmol, 50 pmol, 200 pmol, and 1000 pmol) in the tubes, respectively, which contained 2.5 μL of 10×T4 DNA ligase buffer (660 mM Tris-HCl, 66 mM MgCl₂, 100 mM DTT, and 1 mM ATP, pH7.6) and appropriate amount of ultrapure water. The total volume of ligation procedure was 25 μL. After 1-h incubation, 1 μL of T4 DNA ligase and 0.5 μL of 0.5% BSA were added into the mixture, and incubated at 37 °C for 2 h. Then, the reaction mixture was inactivated at 65 °C for 12 min. The resultant CTs, with different ligation efficiency caused by different ratio of Template and HCV, were stored at 4 °C. Then, 5 μL of CTs with different ligation efficiency were introduced into the solution respectively, in which 5 μL of 2 units/μL Phi29 DNA polymerase, 10 μL of 10×Phi29 DNA polymerase buffer (50 mM Tris-HCl, 10 mM MgCl₂, 10 mM (NH₄)₂SO₄, and 4 mM DTT, pH7.5), 10 μL of 10 mM dNTPs, 2 μL of 0.5% BSA, and appropriate amount of ultrapure water were included, to initiate the RCA reaction. The total volume of RCA procedure was 100 μL.

For the monitoring of RCA process, 5 μL of RCA solutions at different reaction time were removed and transferred into the 96-well microplate. After introducing 5 μL of the above UiO-66-NH₂ suspension and 90 μL of ultrapure water, fluorescence measurements were performed by the BioTek Microplate Reader, and visual readouts were achieved by naked eye under 365 nm light.

12. DNA oligonucleotides

In this work, DNA oligonucleotides were synthesized and purified by Sangon Biotech. Co., Ltd. (Shanghai, China). The detailed sequences were shown in Table S3. DNA powders were dissolved and diluted with ultrapure water ($\geq 18.2 \text{ M}\Omega \text{ cm}^{-1}$) and

stored at -20°C. Estimation of the melting temperature (T_m) and delta G of hybrid was calculated by the IDT Oligo Analyzer and evaluation of the reaction between oligonucleotides was also simulated by NUPACK.

Table S3. Sequences of all DNA oligonucleotides used in this work

Name	Sequence (5' - 3')
HCV	TAG CGT TGG GTT GCG AAA GGC CTT GT
Template	TCG CAA CCC CTC TAT GCA GAC AGC AGC GTT ATT ATT ATT ATT ACA GAC AGC AGC GTT ATT TAT TAT TTA TTG GTA CGA CAA GGC CTT

13. Size effect of UiO-66-NH₂

To explore the size effect, UiO-66-NH₂ with different diameters were synthesized by dielectric barrier discharge plasma, and characterized by PXRD and SEM. The results (Figure S7) indicate the successful synthesis of UiO-66-NH₂ with the average diameters of around 138 nm, 195 nm and 250 nm, respectively.

And then, different concentrations of PPI (2 μM, 5 μM, 10 μM, 20 μM, 50 μM, 100 μM and 200 μM) were tested by these UiO-66-NH₂ with different sizes. Recorded the fluorescence recovery by the BioTek Microplate Reader, and calculated the corresponding LOD of UiO-66-NH₂ with each size, based on $3\delta/\text{slope}$. The results in Figure S8 demonstrated that there was no significant difference between these UiO-66-NH₂ with different sizes, on the PPI detection in terms of dynamic range, slope and LOD.

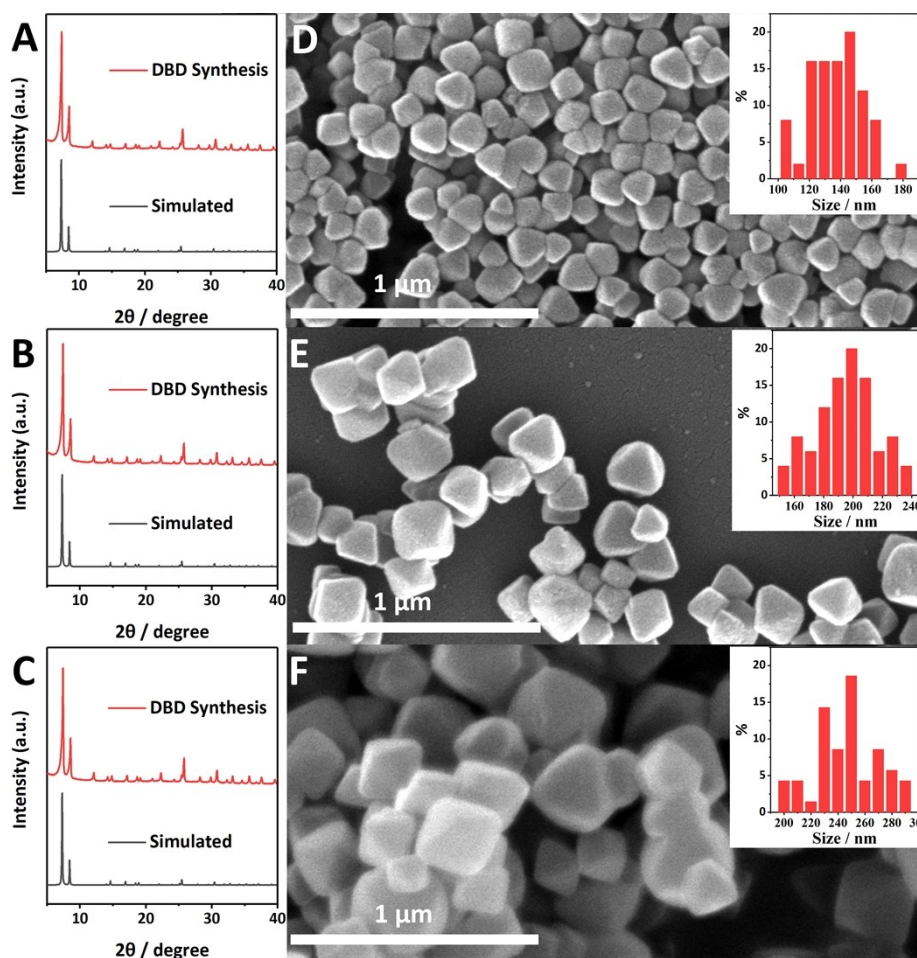


Figure S7. Characterization of UiO-66-NH₂ from DBD plasma-induced synthesis. (A) PXRD pattern and (D) SEM imaging of UiO-66-NH₂ with smaller size. (B) PXRD pattern and (E) SEM imaging of UiO-66-NH₂ with medium size. (C) PXRD pattern and (F) SEM imaging of UiO-66-NH₂ with larger size. The inserts represent corresponding size distribution of each UiO-66-NH₂.

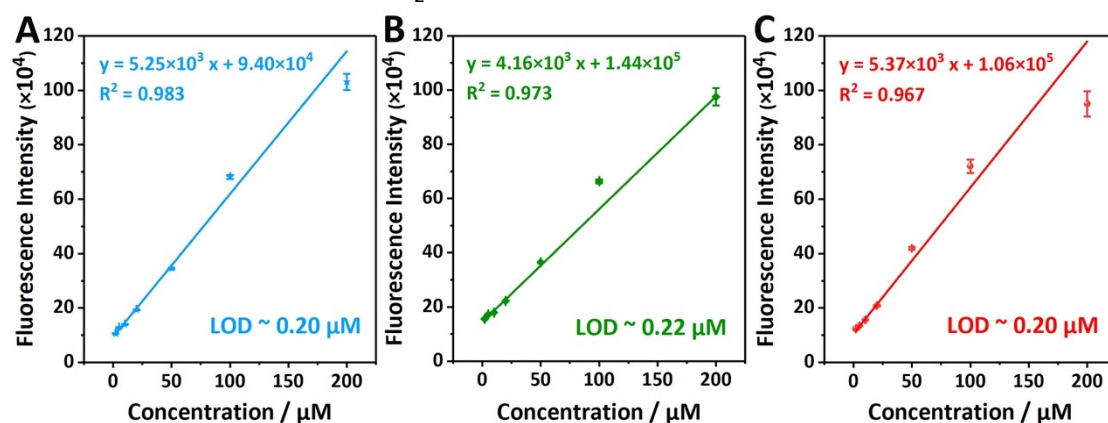


Figure S8. Analytical performance of UiO-66-NH₂ with the average diameters of (A) 138 nm, (B) 195 nm, (C) 250 nm, for PPI detection.

Furthermore, the real-time fluorescence response and reproducibility of UiO-66-NH₂ with different diameters, were also recorded. The real-time fluorescence recovery exhibited the similar trends between UiO-66-NH₂ with different sizes, which reached the equilibrium after about 60 min (Figure S9). Besides, reproducibility tests demonstrated that the behavior of UiO-66-NH₂ with different sizes did not change significantly, thus indicating the high reproducibility (Figure S10).

Therefore, the different sizes of UiO-66-NH₂ did not have a significant effect on the analytical sensing performance. Even if the sizes of the synthesized UiO-66-NH₂ were not completely equal, they did not adversely affect their sensing results, and this also demonstrated the advantage of great stability when applied to the fluorescence tracking of nucleic acid amplification process.

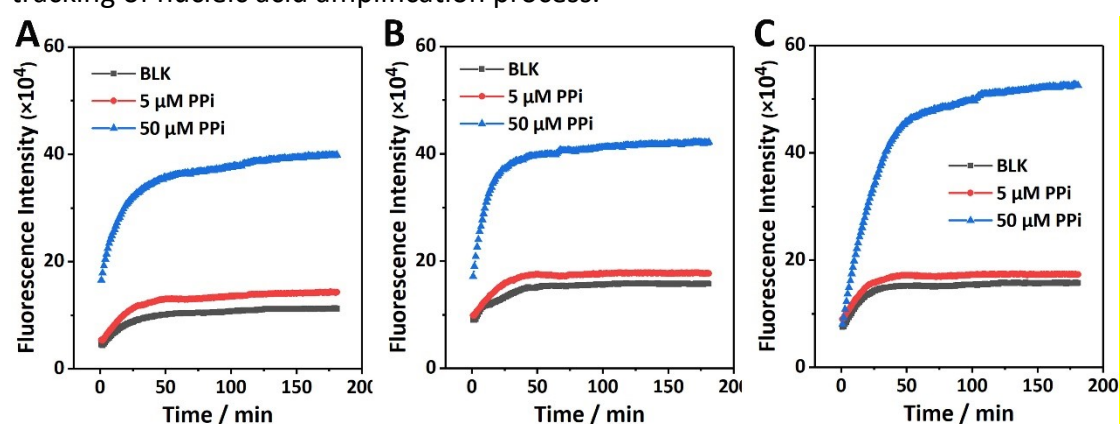


Figure S9. The real-time fluorescence response of UiO-66-NH₂ to PPI, with average diameters of around (A) 138 nm, (B) 195 nm, and (C) 250 nm.

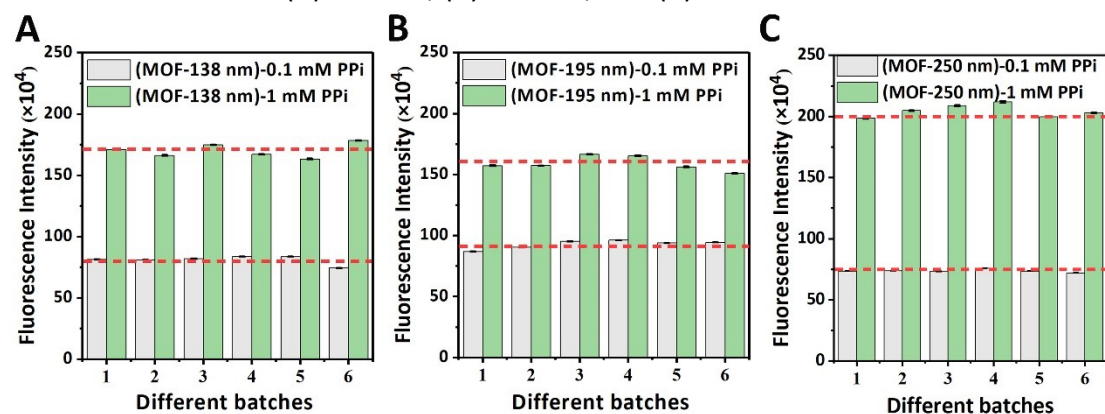


Figure S10. Reproducibility tests of UiO-66-NH₂ with the average diameters of around (A) 138 nm, (B) 195 nm, and (C) 250 nm.

14. Optimization of UiO-66-NH₂ suspension

The concentration of UiO-66-NH₂ suspension is directly related to the signal output of RCA process monitoring. Therefore, different concentrations of UiO-66-NH₂ suspension were individually tested, including 10 mg/mL, 20 mg/mL, 50 mg/mL, 100

mg/mL, 200 mg/mL, 500 mg/mL, and 1000 mg/mL. The fluorescence response to the same PPI climbed gradually along the increasing amount of UiO-66-NH₂, reaching to the highest signal to noise ratio with 50 mg/mL UiO-66-NH₂, and then declined to almost 0 with the continuously increasing amount of UiO-66-NH₂.

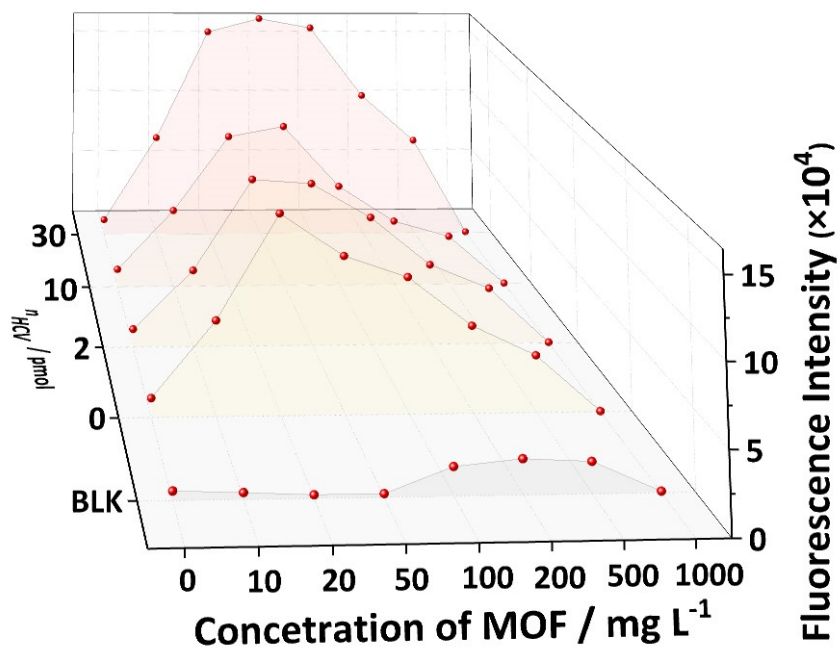


Figure S11. Optimization of concentration of UiO-66-NH₂ suspension.

15. Detection of PPI in RCA process initiated by different concentration of padlock

Table S4. Protocol for the detection of PPI in RCA process

No.	HCV	Template	T4 Ligase	Phi29 DNA polymerase	dNTP	UiO-66-NH ₂
1	0 pmol					
2	2 pmol					
3	10 pmol		350 U/ μ L	10 U/ μ L	10 mM	1 mg/mL
4	50 pmol	200 pmol				
5	200 pmol		1 μ L	1 μ L	10 μ L	5 μ L
6	1000 pmol					

To evaluate the capability of UiO-66-NH₂ for RCA process monitoring, different concentrations of HCV was introduced to initiate RCA with the existence of Phi 29 DNA polymerase and dNTP. 2-h incubation ensured adequate RCA process and PPI releasing. The detailed protocol was shown in Table S4. The RCA products (white floc) was characterized by EDS elemental mapping (Figure S12), which exhibited obvious signals of P, C and O, presumably from DNA.

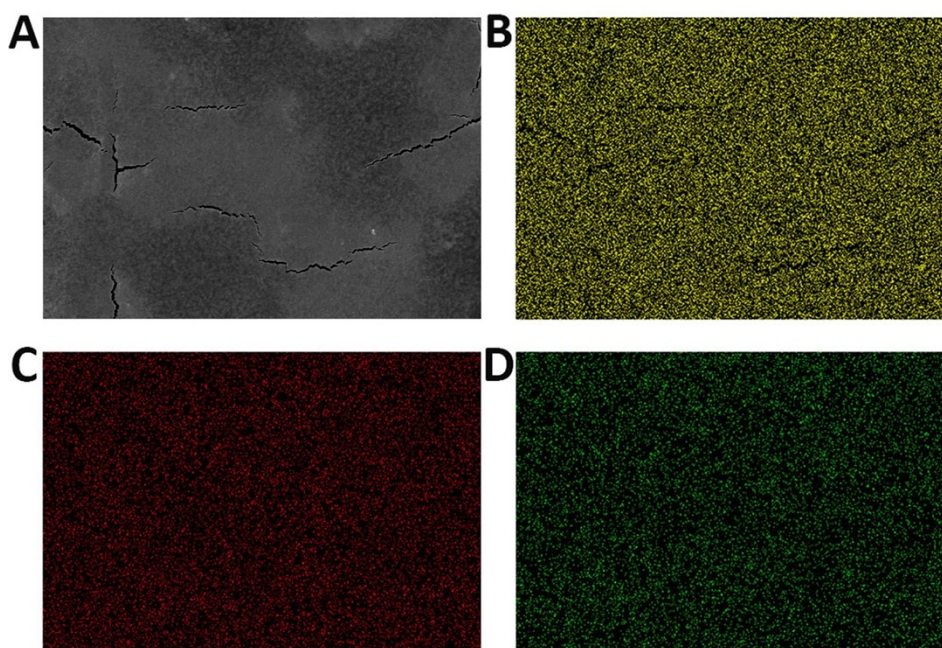


Figure S12. EDS characterization of RCA product. (A) SEM imaging, and the corresponding elemental mapping of (B) P, (C) C, and (D) O.

16. Detection of PPI in RCA solutions from different reaction time

Table S5. Protocol for the RCA process monitoring

No.	Reaction time	HCV	Template	T4 Ligase	Phi29 DNA polymerase	dNTP	UiO-66-NH ₂
1	0						
2	10 min						
3	20 min						
4	30 min						
5	40 min	10 pmol		350 U/ μ L	2 U/ μ L	10 mM	1 mg/mL
6	50 min	/200 pmol	200 pmol	1 μ L	5 μ L	10 μ L	5 μ L
7	60 min						
8	80 min						
9	100 min						
10	120 min						

To further explore the possibility of RCA process monitoring, RCA solutions from different reaction time were mixed with UiO-66-NH₂ suspension (Table S5). With the progress of the reaction, dNTP was gradually consumed to produce PPI, which made the fluorescence of MOF gradually recovered (Figure S13).

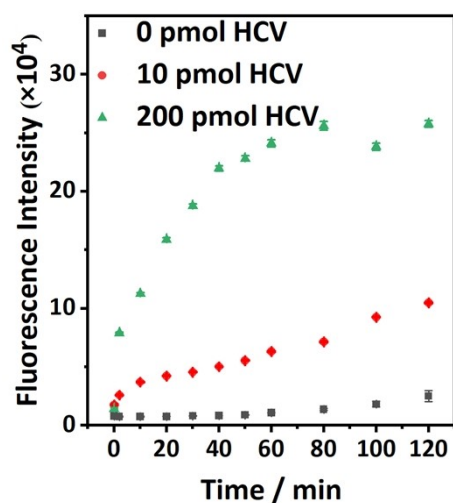


Figure S13 Fluorescence intensity of UiO-66-NH₂ for the detection of RCA process at different time, which was initiated by 10 pmol HCV and 200 pmol HCV individually.

17. Morphological characterization of UiO-66-NH₂ after reaction

To further verify that coordination of PPI would not destroy the framework structure of UiO-66-NH₂, SEM was applied to characterize UiO-66-NH₂ after reaction with PPI. The SEM imaging in Figure S14 illustrated that UiO-66-NH₂ retain its octahedral structure, which confirmed our statement.

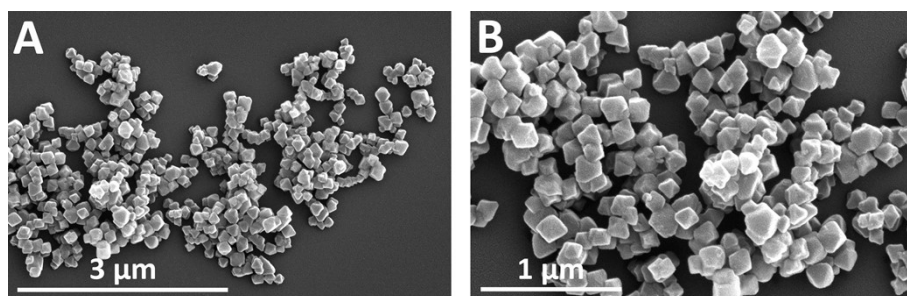


Figure S14. SEM imaging of UiO-66-NH₂ after reaction with PPI, remaining the same octahedral particles.

18. Reproducibility of UiO-66-NH₂

To estimate the stability and reproducibility of UiO-66-NH₂, fluorescence recovery of UiO-66-NH₂ response to different concentrations of PPI and RCA solution initiated by different moles of HCV, were recorded once a day during a week, respectively. An upward trend was seen with the rise of PPI concentration (added or released from RCA process), and the fluorescence intensity of each batch remained constant over this period (Figure S15). The above results demonstrated that UiO-66-NH₂ possessed great stability and reproducibility.

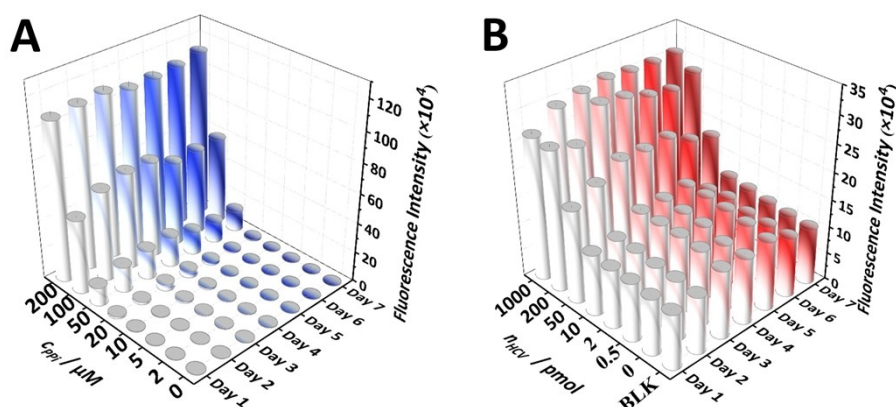


Figure S15. Fluorescence measurement of UiO-66-NH₂ response to (A) PPI added directly and (B) PPI released from RCA process throughout a week.

References

1. H. Yu and D. Long, *Microchimica Acta*, **2016**, *183*, 3151-3157.
2. L. Qin, X. Wang, Y. Liu and H. Wei, *Anal. Chem.*, **2018**, *90*, 9983-9989.
3. C. Wang, G. Tang and H. Tan, *J. Mater. Chem. B*, **2018**, *6*, 7614-7620.
4. H. Li, J. Ren, X. Xu, L. Ning, R. Tong, Y. Song, S. Liao, W. Gu and X. Liu, *Analyst*, **2019**, *144*, 4513-4519.
5. X. An, Q. Tan, S. Pan, H. Liu and X. Hu, *Spectrochim. Acta A Mol. Biomol. Spectrosc.*, **2021**, *247*, 119073.
6. A. Helal, M. E. Arafat and M. M. Rahman, *Chemosensors*, **2020**, *8*, 122.